

1 **Necrotizing Soft Tissue Infections *Staphylococcus aureus* - but**  
2 **not *Streptococcus pyogenes*- isolates display high rate of**  
3 **internalization and cytotoxicity toward human myoblasts**

4  
5 Jessica Baude<sup>1</sup>, Sylvère Bastien<sup>1</sup>, Yves Gillet<sup>1,2</sup>, Pascal Leblanc<sup>3</sup>, Andreas  
6 Itzek<sup>4</sup>, Anne Tristan<sup>1,2</sup>, Michèle Bes<sup>1,2</sup>, Stephanie Duguez<sup>5</sup>, Karen Moreau<sup>1</sup>, Binh  
7 An Diep<sup>7</sup>, Anna Norrby-Teglund<sup>8</sup>, Thomas Henry<sup>1</sup>, François Vandenesch<sup>1,2</sup>, and  
8 INFECT Study Group.

9  
10 1 CIRI, Centre International de Recherche en Infectiologie, Université de Lyon;  
11 Inserm U1111; Ecole Normale Supérieure de Lyon; Université Lyon 1 ; CNRS,  
12 UMR5308; Hospices Civils de Lyon ; Lyon, France.

13 2 Centre National de Référence des Staphylocoques, Institut des Agents  
14 Infectieux, Hospices Civils de Lyon, Lyon, France

15 3 NeuroMyoGene Institute, Université de Lyon, CNRS UMR5310, INSERM  
16 U1217, Lyon, France

17 4 Helmholtz-Zentrum für Infektionsforschung GmbH | Inhoffenstraße 7 | 38124  
18 Braunschweig

19 5 Northern Ireland Center for Stratified Medicine, Biomedical Sciences  
20 Research Institute, Londonderry, UK

21 6 Centre de biotechnologie cellulaire et Biothèque, Groupe Hospitalier Est,  
22 Hospices Civils de Lyon, 69677 Bron, France

23 7 Division of HIV, Infectious Diseases, and Global Medicine, Department of  
24 Medicine, University of California, San Francisco, California, USA

25 8 Center for Infectious Medicine, Karolinska Institutet, Karolinska University  
26 Hospital | Alfred Nobels Allé 8 | 141 52 Huddinge, Sweden

27

28 [jessica.baude@univ-lyon1.fr](mailto:jessica.baude@univ-lyon1.fr)

29 sylvere.bastien@inserm.fr

30 yves.gillet@chu-lyon.fr

31 pascal.leblanc@univ-lyon1.fr

32 andreas.itzek@live.de

33 anne.tristan@chu-lyon.fr

34 michele.bes@chu-lyon.fr

35 s.duguez@ulster.ac.uk

36 karen.moreau@univ-lyon1.fr

37 binh.diep@ucsf.edu

38 anna.norrby-teglund@ki.se

39 thomas.henry@inserm.fr

40 francois.vandenesch@univ-lyon1.fr

41

42 Corresponding author: francois.vandenesch@univ-lyon1.fr

43

44 **Abstract (250 words)**

45

46 Necrotizing Soft Tissue Infections (NSTIs), often reaching the deep fascia and  
47 muscle, are mainly caused by group A *Streptococcus* (GAS) and to a lesser  
48 extent by *Staphylococcus aureus* (SA). Conversely SA is a leading etiologic  
49 agent of pyomyositis suggesting that SA could have a specific tropism for the  
50 muscle. To assess the pathogenicity of these two bacterial species for muscles  
51 cells in comparison to keratinocytes, adhesion and invasion of NSTI-GAS and  
52 NSTI-SA were assessed on these cells. Bloodstream infections (BSI) SA  
53 isolates and non-invasive coagulase negative Staphylococci (CNS) isolates  
54 were used as controls.

55 SA isolates from NSTI and from BSI exhibited stronger internalization into  
56 human keratinocytes and myoblasts than CNS or NSTI-GAS. While the median  
57 level of SA internalization culminated at 2% in human keratinocytes, it reached  
58 over 30% in human myoblasts due to a higher percentage of infected myoblasts  
59 (>11%) as compared to keratinocytes (<3%) assessed by transmission electron  
60 microscopy. Higher cytotoxicity for myoblasts of NSTI-SA as compared to BSI-  
61 SA, was attributed to higher levels of *psm $\alpha$*  and *RNAIII* transcripts in NSTI group  
62 as compared to hematogenous group. However, the two groups were not  
63 discriminated at the genomic level. The cellular basis of high internalization rate  
64 in myoblasts was attributed to higher expression of  $\alpha 5\beta 1$  integrin in myoblasts  
65 as compared to keratinocytes. Major contribution of FnbpAB-integrin  $\alpha 5\beta 1$   
66 pathway to internalization was confirmed by isogenic mutants.

67 Our findings suggest the contribution of NSTI-SA severity by its unique  
68 propensity to invade and kill myoblasts, a property not shared by NSTI-GAS.

69

70 **Importance (150 word)**

71 Necrotizing Soft Tissue Infection (NSTI) is a severe infection caused mainly by  
72 group A *Streptococcus* (GAS) and occasionally by *S. aureus* (SA); the latter  
73 being more often associated with pyomyositis. NSTIs frequently involve the  
74 deep fascia and may provoke muscle necrosis. The goal of this study was to  
75 determine the tropism and pathogenicity of these two bacterial species for  
76 muscle cells. The results revealed a high tropism of SA for myoblasts and  
77 myotubes followed by cytotoxicity as opposed to GAS that did not invade these  
78 cells. This study uncover a novel mechanism of SA contribution to NSTI with a  
79 direct muscle involvement, while in GAS NSTI this is likely indirect, for instance,  
80 secondary to vascular occlusion.

## 81 **Introduction**

82

83 Necrotizing fasciitis and other necrotizing soft tissue infections (NSTIs) are the  
84 most extreme development of skin and soft tissue infections, requiring intensive  
85 care and surgical removal of necrotic tissues. NSTI encompass various clinical  
86 entities (1, 2). They are characterized anatomically by necrotic infections  
87 beyond the subcutaneous tissue and the superficial fascia, often involving the  
88 deep fascia and sometimes associated with myonecrosis (2). Based on the  
89 polymicrobial or monomicrobial character of the infection, NSTIs are classified  
90 as type I and type II, respectively. Type I is a polymicrobial infection involving  
91 aerobic and anaerobic organisms and, depending of the study, is either less or  
92 equally prevalent to type II (1). Type II is a monomicrobial infection caused by  
93 group A Streptococcus (GAS) and to a lesser extent by *Staphylococcus aureus*  
94 (SA), notably methicilin-resistant *S. aureus* (MRSA) (3). Although SA is a  
95 common cause of superficial SSTI and cellulitis (4), the exact prevalence of SA  
96 in NSTI is difficult to assess, principally because of the lack of prospective  
97 controlled population-based studies. Myositis has been reported as “an  
98 unexpected finding” in SA NSTI cases (3) and SA is typically an agent of  
99 pyomyositis, notably in tropical countries (5–8). Altogether, these  
100 epidemiological reports suggest a particular tropism and pathogenesis of SA for  
101 the skeletal muscles. The aim of the present study was to investigate and  
102 compare the invasiveness of muscle cells by SA and GAS as the two major  
103 species responsible for type II NSTI. We showed that SA displays a unique

104 propensity to invade muscle cells principally via the FnbpAB-integrin  $\alpha 5\beta 1$   
105 pathway, a property that is not seen in GAS from NSTI patients.

## 106 **Results**

107 **SA display enhanced internalization rate in myoblasts as compared to**  
108 **other species.** The capacity of both SA and GAS isolates to adhere and invade  
109 keratinocyte or myoblasts was evaluated using a gentamicin protection assay.  
110 NSTI-SA and bloodstream infections (BSI-SA, used as non-NSTI invasive  
111 infections controls) exhibited stronger adhesion than non-invasive coagulase  
112 negative Staphylococci (CNS) or NSTI-GAS, onto human keratinocytes (Fig  
113 1A). Internalization into keratinocytes was also significantly higher for NSTI-SA,  
114 as compared to the other groups, although the frequencies of infected cells were  
115 relatively low (mean 2%) (Fig 1B). Adhesion on and internalization into murine  
116 and human myoblasts showed contrasting results. While there were no  
117 significant differences between NSTI-SA and NSTI-GAS in adhesion on murine  
118 and human myoblasts (Fig 2A and 2B), a dramatic difference in internalization  
119 rate was observed, reaching 30-40% for SA (NSTI and BSI) and only 1-5% for  
120 NSTI-GAS (Fig 2C and 2D). This very high level of internalization into murine  
121 and human myoblast is unique to SA and is shared by all SA strains of the  
122 present study. To determine if this high internalization level was caused by a  
123 higher mean number of infected cells or by a higher mean number of bacteria  
124 per cells, transmission electron microscopy (TEM) was performed on human  
125 myoblasts and keratinocytes upon infection by one NSTI-SA (INFECT2127)  
126 strain and one SA reference strain (SF8300). The results revealed that the mean  
127 number of bacteria per infected cells (actually TEM section) was equivalent in  
128 myoblast and keratinocytes (average 3-4 bacteria per infected cell) (Table 1).

129 Conversely the percentage of infected cells was significantly higher in human  
130 myoblast (14.62 and 11.43% for INFECT2127 and SF8300, respectively) as  
131 compared to keratinocytes (2.86 and 1.43% for INFECT2127 and SF8300,  
132 respectively), which is in the order of magnitude of the difference in  
133 internalization rates between the two cell types as observed by gentamycin  
134 protection assay.

135

136 **The high rate of SA invasion into muscle cells is not an artifact of**  
137 **immaturity.** To rule out the possibility that the observed phenotype in myoblasts  
138 could be an artifact of immature cells, the same experiments were performed in  
139 myoblast-derived myotubes. Maturity of the cells was assessed morphologically  
140 and also by the occurrence of contractibility under video microscopy (Movie S1-  
141 S2). In these conditions, the level of internalization of NSTI-SA and BSI-SA was  
142 29.7% and 27.5% respectively, and thus not different to that obtained in  
143 myoblasts with the same strains (34.8% and 25.7% for NSTI-SA and BSI-SA  
144 respectively) (Fig. S1). These data indicate that the high internalization rate of  
145 SA is a shared property of the myoblastic lineage.

146

147 **FnbpAB is the major determinant of SA internalization into myoblast.** To  
148 determine which *S. aureus* surface proteins are involved in SA internalization  
149 within myoblast, mutant strains for the genes encoding the main effectors of SA  
150 internalization, namely, FnbpAB, ClfA, Atl, SdrD, Tet38 and Gap (Table S1) (9),  
151 excluding those not present in all our SA strains (Eap), were tested. The results



152 revealed a major contribution of FnbpAB. Indeed, while the single *fnbA* and B  
153 mutants had no significant phenotype, the double mutant delta-*fnbAB* was  
154 internalized 1000-fold less (internalization reduced by 99.999%) than the wild  
155 type (WT) strain (Fig. 3). The major impact of FnbpAB was confirmed by using  
156 another *fnbAB* double mutant in strain 8325-4 (DU5883) (not shown). Other  
157 adhesins also contributed to some extent to internalization into myoblast:  
158 mutants in *atl*, *gap*, *clfA* and *tet38* were impaired in internalization by 71%,  
159 27.4%, 25% and 24.6 %, respectively, as compared to the WT strain. (Fig. 3).

160

161 **Myoblasts express increased level of Integrin  $\alpha 5\beta 1$ .** To investigate the  
162 cellular basis of high internalization rate of SA in myoblasts (ca 30-40%) as  
163 compared to keratinocytes (ca 2%), we analyzed the expression of integrin  $\alpha 5\beta 1$   
164 (the major target of FnbpAB internalization pathway) on human keratinocyte and  
165 myoblasts. Flow cytometry analysis by using an anti- $\alpha 5\beta 1$  antibody showed a  
166 greater expression of the  $\alpha 5\beta 1$  integrin at the surface of myoblasts as compared  
167 to keratinocytes (Fig. 4A). Next, the transcription of integrin  $\alpha 5\beta 1$  as well as  
168 other eukaryotic surface receptors involved in *S. aureus* internalization (9) was  
169 evaluated by RT-qPCR in the two cell lines. The integrin  $\alpha 5\beta 1$  displayed  
170 contrasting results: whilst integrin  $\beta 1$  was expressed at the same level in both  
171 cell lines, integrin  $\alpha 5$  was expressed three times more in myoblasts. The  
172 expression of integrin  $\beta 1$  was at least 20 times higher than integrin  $\alpha 5$ ,  
173 implicating integrin  $\alpha 5$  as the limiting partner of the heterodimer (Fig. 4B).  
174 Altogether, flow cytometry and RT-qPCR results suggest that functional  $\alpha 5\beta 1$  is

175 expressed at higher level in myoblasts as compared to keratinocytes. Finally,  
176 the major role of integrin  $\alpha 5\beta 1$  pathway for SA internalization into myoblasts was  
177 confirmed by preincubation of cells with anti- $\alpha 5\beta 1$  antibodies before being  
178 challenged by SA, which reduced internalization by more than 65% (Fig. S2).  
179 In addition, the transcription of all other cellular receptors known to be involved  
180 in SA internalization (Integrin $\alpha V$ , Integrin $\beta 3$ , Hsc70, Annexin 2, Hsp60, CD36,  
181 gp340) (9) was studied. Increased expression tendency was generally observed  
182 in myoblast as compared to keratinocytes (Fig. S3). Altogether, these results  
183 strongly suggest that the higher internalization of SA in myoblast compared to  
184 keratinocytes is mediated by various pathways with a preeminence of the FnBP-  
185 Fibronectin- $\alpha 5\beta 1$  integrin-mediated pathway.

186

187 **Intracellular *RNAIII* and *psmA* transcript levels correlate with cytotoxicity**  
188 **of NSTI-SA.** Since the level of internalization in a given cell type does not inform  
189 about the fate of internalized bacteria (i.e. dormancy versus cytotoxicity), the  
190 toxicity associated with bacterial internalization was estimated at 24h post-  
191 infection by the lactate dehydrogenase (LDH) quantification. NSTI-SA and BSI-  
192 SA were as cytotoxic as GAS on keratinocytes; of note CNS were significantly  
193 less cytotoxic toward this cell line than other bacterial groups. The most  
194 noticeable cytotoxic effect of NSTI-SA was observed on murine and human  
195 myoblasts as compared to all other groups, namely NSTI-GAS, CNS, and  
196 unexpectedly BSI-SA. (Fig. 5). Of note, the culture supernatant from SA and  
197 GAS cultures did not produce cytotoxicity on keratinocytes and myoblasts (Fig

198 S4), assessing that the observed cytotoxicity was not caused by toxins or other  
199 products released by the bacteria. To elucidate the basis of higher cytotoxicity  
200 for myoblasts of NSTI-SA as compared to BSI-SA, the level of the major  
201 effectors of intracellular *S. aureus* cytotoxicity, namely PSM $\alpha$ , Hla, Ldh and Agr-  
202 RNAIII (10, 11) were assessed by RT-qPCR. The levels of *RNAIII* and *psm $\alpha$*   
203 were significantly higher in NSTI-SA strains as compared to BSI-SA in  
204 intracellular conditions into human myoblasts (Fig. 6) as well as from planktonic  
205 culture (data not shown). In contrast, the level of *hla* and *ldh* transcript were not  
206 significantly different between the two groups.

207

208 **Differences in cytotoxicity between NSTI-SA and BSI-SA is not resolved at**  
209 **the genomic level.**

210 In order to confirm that the differences between NSTI-SA and BSI-SA isolates  
211 in *RNAIII* and *psm $\alpha$*  expression were not related to a genomic bias, a genomic  
212 analysis was conducted on the 30 *S. aureus* strains. Phylogenetic analysis  
213 based on core-genome confirmed that NSTI and hematogenous strains were  
214 phylogenetically entangled (Fig. S5). Virulence factor distribution assessed by  
215 micro-array or WGS was not contributive to distinguish NSTI-SA from BSI-SA  
216 isolates (Table 2). Notably, there was no virulence factors discriminating the two  
217 groups. Detailed genomic could not identify discriminant marker between the  
218 two groups either considering genomic determinants presence/absence  
219 (including ncRNA, virulence genes,...) or single nucleotide polymorphism  
220 (SNPs) (Text. S1).

## 221 Discussion

222

223 Necrotizing fasciitis is a rare disease that involves superficial fascia and results  
224 in the extensive damage and necrosis of the surrounding tissue including  
225 muscle. In the present study we show that SA may contribute to this disease by  
226 its unique propensity to invade muscle cells and consequently trigger cell death,  
227 a property that is not seen in GAS from NSTI patients. Interestingly, this unique  
228 capacity of *S. aureus* to invade myoblast and myotube from both mice and  
229 human origin is uncommon, as neither CNS nor GAS did internalize in those  
230 cells to such efficiency. Moreover, to our knowledge, there is no other type of  
231 eukaryotic cells in which SA internalizes at this level (over 30%), e.g. the level  
232 of SA internalization is ca. 17% in human embryonic kidney cells (12), 8% in  
233 endothelial cells (12), 2% in human alveolar epithelial cells (A549) (K. Moreau,  
234 unpublished data), <1% HELA epithelial cells (13), <1% within osteoblast (14)  
235 and <2% in osteoclast (15). We could demonstrate that this high rate of  
236 internalization depends on several of the known pathways of *S. aureus*  
237 internalization with a preeminence of the FnBP-Fibronectin- $\alpha 5\beta 1$  integrin-  
238 mediated pathway. The increased expression at the surface of human  
239 myoblasts of  $\alpha 5\beta 1$  integrin and other known receptors involved in SA  
240 internalization (integrin  $\alpha V$  and  $\beta 3$ , HSC70, Annexin 2, Hsp60, CD36 and  
241 Gp340) is a likely explanation for the high internalization rate of SA within  
242 myoblasts as compared to keratinocytes. This model is also consistent with TEM  
243 observation of a higher percentage of infected cells as compared to

244 keratinocytes. The direct consequence of this high rate of internalization within  
245 myoblast is a higher cytotoxicity to these cells, and not, as observed in other  
246 setting a reduced cytotoxicity associated with high internalization rate (11).

247 Virulence factors that could be associated with NSTI-SA have been largely  
248 debated, Panton Valentine Leucocidin being frequently reported in US studies  
249 involving community-acquired MRSA USA300 (3). Other cases associated with  
250 *tst*- (16) or with *egc*-encoding isolates were reported (17), reminiscent of the  
251 involvement of superantigens in severe GAS tissue infections (18). Noticeably,  
252 the 9 NSTI-SA strains of the present study were not clonally related; none of  
253 these were MRSA and a single one was PVL-positive (Table 2). Their genetic  
254 content regarding virulence factors including superantigens was not significantly  
255 different from the BSI-SA strains that represent another major invasive disease  
256 (Table 2). WGS comparison by multiple approaches could not discriminate the  
257 two diseases isolate groups (Text S1). This lack of discrimination might be  
258 caused by the small size of the NSTI group leading to insufficient statistical  
259 power. However, the observation that BSI-SA were less cytotoxic than NSTI-SA  
260 with similar internalization rate (Fig. 5), is in accordance with previous studies  
261 showing that skin and soft tissue infection isolates produce more PSM $\alpha$  (as  
262 observed in our study with NSTI isolates) than infective endocarditis or hospital-  
263 acquired pneumonia isolates (19). This is also reminiscent of previous  
264 observation suggesting an association between low-toxicity and bacteraemia  
265 (20): It has been hypothesized that such invasive bloodstream infections limit  
266 the opportunities for onward transmission, whilst highly toxic strains associated

267 with skin infections could gain an additional between-host fitness advantage,  
268 potentially contributing to the maintenance of toxicity at the population level (20).  
269 Altogether this analysis reveal that despite similar virulence factor repertoire,  
270 NSTI-SA and BSI-SA isolates differ in their phenotypic expression of virulence  
271 and may thus be considered as different pathovars.

272 The respective contribution of GAS and SA to NSTI is a matter of debate. Of  
273 note, the four strains of GAS isolated from NSTI patients, despite being isolated  
274 from very severe cases of NSTI, did not present a strong invasive capacity for  
275 muscle cells *in vitro*. This result is counter-intuitive given the involvement of  
276 epidermis, dermis, subcutaneous tissue, fascia, and muscle in GAS-NSTI (1).  
277 This suggests that the muscle involvement in GAS NSTI does not result from  
278 bacterial invasion of muscle cells whilst it could be the cases for SA-NSTI when  
279 muscle involvement occurs as described (3). However, if the muscle destruction  
280 seen in GAS-NSTI is not caused by direct intracellular toxicity of GAS, it is likely  
281 not caused either by the toxicity of secreted enzymes and toxins for the muscle  
282 cells, as culture supernatant neither from GAS nor from SA had any significant  
283 toxicity on cultured myoblasts. It is thus more likely that muscle necrosis in GAS-  
284 NSTI results from vascular occlusion secondary to platelet-leukocytes  
285 aggregation in response to infection of the adjacent anatomical skin and soft  
286 tissue structures.

287 In conclusion, our results uncover new insight into the pathophysiology of GAS  
288 and SA-NSTI and provide a new cellular basis for the contribution of *S. aureus*

289 to pathogenesis of NSTI and other deep-seated infection involving the muscle.  
290 It also sustains the potential synergy of GAS and SA in NSTI, a situation that is  
291 not uncommon (2, 21). It advocates for future prospective clinical study  
292 systematically depicting the anatomical tissue layers of infection according to  
293 the micro-organisms.

## 294 **Material and Methods**

295

### 296 **Ethics statement**

297 Muscle biopsies for myoblast cell line were obtained from the Bank of Tissues  
298 of Research (Myobank BTR, a partner in the EU network EuroBioBank) in  
299 accordance with European recommendations and French legislation. Muscle  
300 biopsies for experiment in primary myoblast were obtained from NeuroBioTec  
301 (Hospices Civils de Lyon, *Centre de Ressources Biologiques*) and declared to  
302 the Ministry of Research under the agreement DC 2011-1437 and the number  
303 of accession AC 2012-1867.

304

### 305 **Bacterial strains**

306 Bacterial isolates are listed in Table 3. They include strains of *S. aureus* (n=4)  
307 and *S. pyogenes* (n=4) isolated from patients included in the INFECT (Improving  
308 Outcome of Necrotizing Fasciitis: Elucidation of Complex Host and Pathogen  
309 Signatures that Dictate Severity of Tissue Infection) cohort which is an  
310 international, prospective, multicenter observational research project (Clinical  
311 Trials #NCT01790698). In addition, 5 *S. aureus* strains from French NSTI  
312 patients spontaneously referred to the French National Reference Laboratory  
313 for Staphylococci were included. The diagnosis of NSTI was made by the  
314 surgeon during the primary operation. It is based on, but not restricted to,  
315 findings of necrosis, dissolved or deliquescent soft tissue, and fascial and  
316 muscular affection (22). The invasive non-NSTI SA control strains consisted in



317 Bloodstream infection (BSI) strains (12 infective endocarditis, 9 bacteremia  
318 without infective endocarditis) collected during a prospective cohort study on *S.*  
319 *aureus* bacteremia (VIRSTA) (23). Those strains were chosen in order to  
320 genotypically match NSTI strains on the basis of micro-array-deduced clonal  
321 complexes (23) confirmed by whole genome sequencing (Illumina MiSeq  
322 technology, Illumina, San Diego, USA, with 16-266 x coverage, median 137).  
323 Non *aureus*-staphylococci were type strains of the most frequently isolated CNS  
324 species. Strains USA300 JE2 and several transposons insertion mutants in  
325 genes encoding proteins potentially involved in internalization (*atl*, *clfA*, *sdrD*,  
326 *tet38*, *gap*, *strA*, *strB*) were retrieved from the public Nebraska library (24) with  
327 substantial help of Ken Bayles. In-frame deletion of the *fnbA*, *fnbB* and double  
328 mutant in the SF8300 background were performed as described previously (25,  
329 26) using the pKOR1 allelic replacement mutagenesis system and the primers  
330 shown in Table S2 in the supplemental material. Laboratory strains and  
331 plasmids are listed in Table S1. All strains were cultured in Brain-Heart infusion  
332 (BHi Becton Dickinson) broth under agitation (200 rpm) at 37°C.

333

334 **Cells and culture conditions.** The human keratinocytes N/TERT-1 cells (27)  
335 were cultured in keratinocyte SFM media (Thermofisher) at 37°C under 5% CO<sub>2</sub>  
336 atmosphere. The murine myoblast cells C2C12 (28) were cultured in Dulbecco's  
337 Modified Eagle's Medium (Thermofisher) supplemented with 20% Fetal Bovine  
338 Serum (Gibco) and 1% penicillin/streptomycin. Murine myoblasts were  
339 differentiated into myotubes by addition of 2% of horse serum (Sigma) in the

340 medium. The human myoblast line was obtained as follows. Deltoid muscle  
341 biopsy from a 71-year-old male was obtained from the Myobank BTR (see  
342 ethical above). Muscle stem cells were extracted, sorted and tested for their  
343 myogenicity as previously described (29). Cells were then expended  
344 in proliferating KMEM medium (1 volume of M199, 4 volumes of  
345 Dulbecco's modified Eagle's medium (DMEM), 20% fetal bovine serum (v/v), 25  
346  $\mu\text{g/ml}$  Fetuin, 0.5 ng/ml bFGF, 5 ng/ml EGF, 5  $\mu\text{g/ml}$  Insulin). The lentiviral  
347 vector particles were produced by transient transfection of the packaging  
348 construct (HIV-1 psPAX2), a minimal genome (HIV-1 pLv-hTERT-CDK4 from  
349 CloneSpace LLC ref SKU: CS1031) bearing the expression cassettes encoding  
350 the Htert and CDK4 proteins and the puromycin resistance, and the VSV-G-  
351 envelope expressing plasmid pMDG2 (DNA ratio 8:8:4  $\mu\text{g}$ ) into 293T cells (3.5  
352  $\times 10^6$  cells plated 1 day before transfection in 100-mm dishes) by the calcium  
353 phosphate method (30). Viral particles were normalized by an exogenous  
354 reverse transcriptase assay and titrated on human primary myoblast cells (31).  
355 Transductions of human primary myoblasts were carried out with different MOI  
356 in 12 well plates (80,000 cells plated 1 day before) in presence of 6  $\mu\text{g/ml}$  of  
357 polybrene overnight in KMEM culture medium as previously described by  
358 Thorley (32). One day after transduction, cells were passaged and cultured in  
359 presence of puromycin (1 mg/ml) during 3-4 days until the death of non-  
360 transduced primary myoblast control cells was completed. Once puromycin  
361 selected, transduced myoblasts were cultured in KMEM-D medium (KMEM  
362 medium with dexamethasone 0.2 mg/ml) in absence of puromycin. After one

363 week of culture in KMEM-D medium, immortalized myoblasts could be cultured  
364 for long term.

365

### 366 **Adhesion, internalization, survival and cytotoxic assays.**

367 The intracellular infection of cells was performed using gentamycin protection  
368 assay as described elsewhere with modifications (33). Cells were seeded at  
369 80,000 cells/well in 24-well plates and incubated at 37°C with 5% CO<sub>2</sub> for 24 h  
370 in culture medium. Bacterial cultures (9h of growth) were washed with PBS and  
371 resuspended in antibiotic-free culture medium at a concentration corresponding  
372 to a MOI of 10. The MOIs were subsequently confirmed by CFU counting upon  
373 agar plate inoculation. Cells were washed twice in PBS to remove antibiotics,  
374 and normalized bacterial suspensions were added to the wells. The infected  
375 cultures were incubated for 2h at 37°C and then washed with PBS. The cells  
376 used to assay invasion were incubated for an additional 1h at 37°C in culture  
377 medium containing 200 mg/L gentamicin and 10 mg/L lysostaphin to rapidly kill  
378 extracellular but not intracellular bacteria. To assay bacterial persistence, the  
379 cultures were further incubated in medium containing 40 mg/L gentamicin and  
380 10 mg/L lysostaphin for 24h. These lower concentrations resulted in the killing  
381 of bacteria cells released upon host cell lysis, thus preventing infection of new  
382 host cells. Cells used to evaluate adhesion (2h post-infection), invasion (3h  
383 post-infection) and persistence (24h post-infection) were lysed by osmotic shock  
384 in sterile pure water, and extensively pipetted to achieve the full release of  
385 bacteria. The bacterial suspension was plated on Trypcase Soy Agar (TSA;

386 bioMérieux, Marcy l'Etoile, France). After 24h of incubation at 37°C, the colonies  
387 were enumerated using an EasyCount automated plate reader (AES  
388 Chemunex). Infected cell death was quantified by the release of the cytosolic  
389 enzyme LDH into the culture supernatant at 24h post-infection using the  
390 CytoTox-ONE Homogeneous Membrane Integrity Assay (Promega) according  
391 to the manufacturer's instructions. LDH release into the supernatant of infected  
392 cells was compared to that of uninfected cells that were either left intact (lower  
393 control) or fully lysed by osmotic shock (higher control). The percentage of  
394 cytotoxicity was calculated as follows:  $((\text{LDH infected cells} - \text{LDH lower control}) / (\text{LDH higher control} - \text{LDH lower control})) \times 100$ .

396

#### 397 **Relative quantification of bacterial RNA by RT-qPCR**

398 Cells lines were infected as described above. After the first antibiotic treatment,  
399 cells and bacteria were harvested by trypsin detachment and centrifugation.  
400 Pellet was treated with 20 µg lysostaphin (1 mg/ml) and RNA isolation was  
401 performed using the RNeasy Plus mini kit (QIAGEN) according to the  
402 manufacturer's instructions. The RNA was quantified using a NanoDrop  
403 spectrophotometer, and 100 ng of total RNA was reverse transcribed into cDNA  
404 using Reverse Transcriptase System (Promega). Two µL of 1/5 diluted cDNA  
405 was used as a template for the real-time PCR amplification using PowerUp  
406 SYBR® Green Master Mix and a StepOne Plus system (Applied Biosystem) with  
407 specific primers shown in Table S2. Genes expression analysis was performed  
408 by using  $\Delta\text{Ct}$  methods using *hu* gene as an internal standard and confirmed by

409 *gyrB* gene.

410

### 411 **Relative quantification of eukaryotic receptors by RT-qPCR.**

412 Total RNA was isolated from CTi400 and N/TERT-1 cells using RNeasy Plus  
413 mini kit (QIAGEN) according to the manufacturer's instructions. Complementary  
414 DNA (cDNA) was synthesized from 1 µg of total RNA using random primers and  
415 Reverse Transcriptase System (Promega). The cDNA was used as a template  
416 for the real-time PCR amplification using PowerUp SYBR® Green Master Mix  
417 and a StepOne Plus system (Applied Biosystem) with specific primers shown in  
418 Table S2. Genes expression analysis was performed by using  $\Delta$ Ct methods  
419 using *β-actin* gene as an internal standard and confirmed by GAPDH.

420

### 421 **Transmission Electron Microscopy**

422 Infected cells were fixed in glutaraldehyde 2% and washed three times in  
423 saccharose 0.4M and sodium cacodylate buffer 0.2M pH 7.4 for 1h at 4°C, and  
424 postfixed with 2% OsO<sub>4</sub> and Na C-HCl Cacodylate 0.3M pH 7.4 30 minutes at  
425 room temperature. Cells were then dehydrated with an increasing ethanol  
426 gradient (5 minutes in 30%, 50%, 70%, 95%, and 3 times 10 minutes  
427 in absolute ethanol). Impregnation was performed with Epon A (50%) plus  
428 Epon B (50%) plus DMP30 (1.7%). Inclusion was obtained by polymerisation at  
429 60°C for 72h. Ultrathin sections (approximately 70 nm thick) were cut on a  
430 ultracut UC7 (Leica) ultramicrotome, mounted on 200 mesh copper grids coated  
431 with 1:1,000 polylysine, stabilized for 1 day at room temperature and, contrasted

432 with uranyl acetate. Sections were examined with a Jeol 1400JEM  
433 (Tokyo,Japan) transmission electron microscope equipped with a Orius 600  
434 camera and Digital Micrograph. Cells were visually examined (175 myoblasts,  
435 455 keratinocytes) to assess the number of infected cells and the number of  
436 bacteria per infected cells.

437

### 438 **Flow cytometry**

439 Cells were trypsinized, washed and suspended in PBS at a concentration of  
440  $1 \cdot 10^6$  per ml, and aliquots were incubated with Fc Block (ThermoFisher  
441 Scientific 14-9161-71) 20 minutes at 4°C. The primary  $\alpha 5\beta 1$  integrin antibody  
442 (10  $\mu\text{g}/\text{mL}$ ) (Merck Millipore MAB1999) was added for 30 minutes at 4°C. Cells  
443 were washed, resuspended in PBS before incubation with Alexa Fluor 647  
444 secondary antibody (10  $\mu\text{g}$  for  $10^6$  cells) (Themofisher Scienfitic A-21236) for 30  
445 minutes at 4°C and then washed 2 times in PBS. Finally, cells were assessed  
446 using a BD Accuri-C6 (BD Biosciences, Le pont de Claix, France) flow  
447 cytometer.

448

### 449 **Statistical analysis**

450 The statistical analyses were performed using GraphPad Prism 6 software. Data  
451 from two groups were compared using either Student's 2-tailed t-test for paired  
452 samples or Mann Whitney test for unpaired samples. Data from more than two  
453 groups were analyzed using multiple pairwise comparisons of the means

454 through a one-way ANOVA including post-hoc tests corrected by a Bonferroni  
455 method. The significance threshold was set at 0.05 for all tests.

456

457

## 458 **Acknowledgments**

459 The authors thank Lam Thuy Hoang, Marine Ibranosyan for help in clinical data  
460 management, Ken Bayles for help in providing Nebraska library mutants, Paul  
461 Verhoven for fruitful discussions, Laurent Schaeffer, Emilie Chopin and Nathalie  
462 Streichenberger from NeuroBio Tec-Banques (Hospices Civils de Lyon, France)  
463 for sharing expertise on muscle cells, CIQLE for technical assistance for  
464 microscopy, Katia Ziadna for all the agar plates and Laurence Cluzeau for  
465 excellent technical support. This work was supported by the EU grant INFECT-  
466 EU-FP7-HEALTH.

467 **Figure legends**

468

469 **Fig. 1. Adhesion and internalization of *Staphylococcus aureus* (SA),**  
470 **coagulase negative *Staphylococcus* (CNS) and group A *Streptococcus***  
471 **(GAS) to human keratinocytes. (A)** Percentages of adhered bacteria were  
472 calculated after 2 hours of infection in relation to inoculum of infection.  
473 Intracellular bacteria assessed in B were subtracted; (B) Internalization was  
474 determined after 2 hours of infection followed by antibiotic treatment to exclude  
475 extracellular bacteria. Multiplicity of infection (MOI) = 10. The horizontal lines  
476 within each group represent the mean value  $\pm$  standard deviations of at least  
477 three independent experiments per strain. \* $p < 0.05$ , \*\* $p < 0.01$ , \*\*\*  $p < 0.001$ .

478

479 **Fig. 2. Adhesion and internalization of *Staphylococcus aureus* (SA),**  
480 **coagulase negative *Staphylococcus* (CNS) and group A *Streptococcus***  
481 **(GAS) to murine and human myoblasts. (A and B)** Percentages of adherent  
482 bacteria were calculated after 2 hours of infection in relation to inoculum of  
483 infection. Intracellular bacteria assessed in C and D were subtracted; (C and D)  
484 Internalization was determined after 2 hours of infection followed by antibiotic  
485 treatment to exclude extracellular bacteria. Multiplicity of infection (MOI) = 10.  
486 The horizontal lines within each group represent the mean value  $\pm$  standard  
487 deviations of at least three independent experiments per strain. \* $p < 0.05$ ,  
488 \*\* $p < 0.01$ , \*\*\*  $p < 0.001$ , \*\*\*\* $p < 0,0001$ .

489



490 **Fig. 3. Internalization of *S. aureus* mutants into human myoblasts.**

491 Internalization of the various mutants in genes encoding surface proteins was  
492 determined after 2 hours of infection followed by antibiotic treatment to exclude  
493 extracellular bacteria. The internalization was normalized to that of wild type  
494 strain. Multiplicity of infection (MOI) = 10. All values are means  $\pm$  standard error  
495 of mean of three independent experiments in duplicate for each strain. \* $p < 0.05$ ,  
496 \*\* $p < 0.01$ , \*\*\*  $p < 0.001$ , \*\*\*\* $p < 0.0001$ .

497

498 **Fig. 4. Expression of  $\alpha 5\beta 1$  integrin by human keratinocyte and myoblasts.**

499 (A) Cell surface expression of  $\alpha 5\beta 1$  integrin assessed by flow cytometry and  
500  $\alpha 5\beta 1$  antibody; (B) Relative transcript levels of  $\alpha 5$ ,  $\beta 1$  integrin sub-units were  
501 determined using quantitative reverse-transcriptase PCR, normalized to the  
502 internal  $\beta$ -actin standard. All values are means  $\pm$  standard error of mean of four  
503 independent experiments.

504

505 **Fig. 5. Cytotoxicity of intracellular bacteria at 24h post infection.**

506 Cytotoxicity was estimated by quantifying LDH release by infected cells at 24  
507 hours post infection. Multiplicity of infection (MOI) = 10. The percentage of  
508 cytotoxicity was calculated as follows:  $((\text{LDH infected cells} - \text{LDH lower control}) / (\text{LDH higher control} - \text{LDH lower control})) \times 100$ . The horizontal lines  
509 within each group represent the mean value  $\pm$  standard deviations of at least  
510 three independent experiments per strain. \* $p < 0.05$ , \*\* $p < 0.01$ , \*\*\*  $p < 0.001$ ,  
511 \*\*\*\* $p < 0.0001$ .

513

514 **Fig. 6. Expression of intracellular bacterial mRNA into human myoblasts**

515 **3 hours post infection.** Relative transcript levels were determined using

516 quantitative reverse-transcriptase PCR and expressed as n-fold change to the

517 internal *hu* standard. The horizontal lines within each group represent the mean

518 value  $\pm$  standard deviations. \* $p < 0.05$ , \*\* $p < 0.01$ .

519

520 **Supplemental material**

521

522 **Movie S1-S2. Murine myotubes.** Mature murine myotubes show spontaneous  
523 contractions.

524

525 **Fig. S1. Comparison of internalization of *Staphylococcus aureus* into**  
526 **murine myotubes and myoblasts.** The murine myoblast cells C2C12 were  
527 cultured in Dulbecco's Modified Eagle's Medium (Thermofisher) supplemented  
528 with 10% Fetal Bovine Serum (FBS) and 1% penicillin/streptomycin. Myoblasts  
529 were differentiated into myotubes by the addition of 2% horse serum in the  
530 medium for eight days. Internalization was determined after 2 hours of infection  
531 followed by antibiotic treatment to exclude extracellular bacteria. Percentage of  
532 numbers of viable bacteria was calculated in relation to infection inoculum.  
533 Multiplicity of infection (MOI) = 10. The diagram represents the mean  $\pm$   
534 standard deviations from three independent experiments of 6 NSTI-SA and 3  
535 BSI-SA.

536

537 **Fig. S2. *Staphylococcus aureus* invasion is mediated by the eukaryotic**  
538 **fibronectin receptor  $\alpha 5\beta 1$  integrin.** Cells preincubated with monoclonal  
539 function-blocking antibodies were challenged with *S. aureus* strain  
540 RN6390 $\Delta$ spA (A. Tristan, Y. Benito, R. Montserret, S. Boisset, E. Dusserre, F.  
541 Penin, F. Ruggiero, J. Etienne, H. Lortat-Jacob, G. Lina, M. Gabriela Bowden  
542 and F. Vandenesch, PLoS ONE 4(4): e5042.

543 doi:10.1371/journal.pone.0005042). This strain was chosen to avoid possible  
544 interference of Fc binding to staphylococcal protein (SpA) present in all *S.*  
545 *aureus* strains. Internalization was determined after 2 hours of infection followed  
546 by antibiotic treatment to exclude extracellular bacteria. Percentage of numbers  
547 of viable bacteria was calculated in relation to infection inoculum. Multiplicity of  
548 infection (MOI) = 10.

549

550 **Fig. S3. Expression of surface receptors in human keratinocytes and**  
551 **myoblasts.** Relative transcript levels were determined using quantitative  
552 reverse-transcriptase PCR, normalized to the internal  $\beta$ -actin standard and  
553 relative expression to human myoblasts. All values are means  $\pm$  standard  
554 deviations of four independent experiments. The statistical significance was  
555 determined by Student's t test with Welch's correction (\*p<0.05).

556

557 **Fig. S4. Cytotoxicity of staphylococcal or streptococcal culture**  
558 **supernatants on murine myoblasts or human keratinocytes.** Bacterial  
559 (NSTI-SA, 6 strains, blue lines; BSI-SA, 3 strains, brown lines; NSTI-GAS, 4  
560 strains, green lines) supernatant (1:50 dilution) was added to the cell culture  
561 medium containing propidium iodide (PI) and cell death was quantified by  
562 monitoring PI incorporation over a 3 hours period. Triton X100 (red line) was  
563 used as positive control. Sterile bacterial culture medium (grey line) and cell  
564 culture medium (black line) were used as negative controls.

565

566 **Fig. S5. Phylogenetic analysis of the *S. aureus* strains.** Rooted phylogenetic  
567 analysis using a maximum likelihood approximation based on the 86233 SNPs  
568 identified through the conserved core genome of the 30 *S. aureus* strains. The  
569 tree is rooted on the clonal complex 1 (MSSA476). NSTI-SA isolates are labeled  
570 in red and BSI-SA in black.

571

572 **Text S1.** Detailed genomic analysis of the 30 *S. aureus* strains.

573

## 574 References

- 575 1. Stevens DL, Bryant AE. 2017. Necrotizing Soft-Tissue Infections. *N Engl J Med*  
576 377:2253–2265.
- 577 2. Rajan S. 2012. Skin and soft-tissue infections: classifying and treating a spectrum.  
578 *Cleve Clin J Med* 79:57–66.
- 579 3. Miller LG, Rieg G, Bayer AS, Spellberg B. 2005. Necrotizing Fasciitis Caused by  
580 Community-Associated Methicillin-Resistant *Staphylococcus aureus* in Los Angeles. *N Engl*  
581 *J Med* 9.
- 582 4. Chira S, Miller LG. 2010. *Staphylococcus aureus* is the most common identified cause  
583 of cellulitis: a systematic review. *Epidemiol Infect* 138:313–317.
- 584 5. Chiedozi LC. Review of 205 Cases in 112 Patients 5.
- 585 6. Christin L, Sarosi GA. 1992. Pyomyositis in North America: Case Reports and  
586 Review. *Clin Infect Dis* 15:668–677.
- 587 7. Hall RL, Callaghan JJ, Moloney E, Martinez S, Harrelson JM. 1990. Pyomyositis in a  
588 temperate climate. Presentation, diagnosis, and treatment. *J Bone Joint Surg Am* 72:1240–  
589 1244.
- 590 8. Hassan FOA, Shannak A. 2008. Primary pyomyositis of the paraspinal muscles: a case  
591 report and literature review. *Eur Spine J Off Publ Eur Spine Soc Eur Spinal Deform Soc Eur*  
592 *Sect Cerv Spine Res Soc* 17 Suppl 2:S239-242.
- 593 9. Josse J, Laurent F, Diot A. 2017. Staphylococcal Adhesion and Host Cell Invasion:  
594 Fibronectin-Binding and Other Mechanisms. *Front Microbiol* 8.
- 595 10. Szafranska AK, Oxley APA, Chaves-Moreno D, Horst SA, Roßlenbroich S, Peters G,  
596 Goldmann O, Rohde M, Sinha B, Pieper DH, Löffler B, Jauregui R, Wos-Oxley ML, Medina  
597 E. 2014. High-resolution transcriptomic analysis of the adaptive response of *Staphylococcus*  
598 *aureus* during acute and chronic phases of osteomyelitis. *mBio* 5.
- 599 11. Rasigade J-P, Trouillet-Assant S, Ferry T, Diep BA, Sapin A, Lhoste Y, Ranfaing J,  
600 Badiou C, Benito Y, Bes M, Couzon F, Tigaud S, Lina G, Etienne J, Vandenesch F, Laurent  
601 F. 2013. PSMs of Hypervirulent *Staphylococcus aureus* Act as Intracellular Toxins That Kill  
602 Infected Osteoblasts. *PLoS ONE* 8:e63176.
- 603 12. Sinha B, Foti M, Hartford OM, Vaudaux P, Foster TJ, Lew DP, Herrmann M, Krause  
604 K-H. 1999. Fibronectin-binding protein acts as *Staphylococcus aureus* invasins via  
605 fibronectin bridging to integrin  $\alpha 5 \beta$ . *Cell Microbiol* 17.
- 606 13. Fowler T, Wann ER, Joh D, Johansson S, Foster TJ, Höök M. 2000. Cellular invasion  
607 by *Staphylococcus aureus* involves a fibronectin bridge between the bacterial fibronectin-  
608 binding MSCRAMMs and host cell  $\beta 1$  integrins. *Eur J Cell Biol* 79:672–679.
- 609 14. Selan L, Papa R, Ermocida A, Cellini A, Ettorre E, Vrenna G, Campoccia D,  
610 Montanaro L, Arciola CR, Artini M. 2017. Serratiopeptidase reduces the invasion of  
611 osteoblasts by *Staphylococcus aureus*. *Int J Immunopathol Pharmacol* 30:423–428.
- 612 15. Trouillet-Assant S, Gallet M, Nauroy P, Rasigade J-P, Flammier S, Parroche P,  
613 Marvel J, Ferry T, Vandenesch F, Jurdic P, Laurent F. 2015. Dual Impact of Live  
614 *Staphylococcus aureus* on the Osteoclast Lineage, Leading to Increased Bone Resorption. *J*  
615 *Infect Dis* 211:571–581.
- 616 16. Omland LH, Rasmussen SW, Hvolris J, Friis-Møller A. 2007. Necrotizing fasciitis  
617 caused by TSST-1 producing penicillinsensitive *Staphylococcus aureus*—a case report. *Acta*  
618 *Orthop* 78:296–297.
- 619 17. Morgan WR, Caldwell MD, Brady JM, Stemper ME, Reed KD, Shukla SK. 2007.  
620 Necrotizing fasciitis due to a methicillin-sensitive *Staphylococcus aureus* isolate harboring an  
621 enterotoxin gene cluster. *J Clin Microbiol* 45:668–671.
- 622 18. Norrby-Teglund A, Thulin P, Gan BS, Kotb M, McGeer A, Andersson J, Low DE.

- 623 2001. Evidence for superantigen involvement in severe group a streptococcal tissue  
624 infections. *J Infect Dis* 184:853–860.
- 625 19. Berlon NR, Qi R, Sharma-Kuinkel BK, Joo H-S, Park LP, George D, Thaden JT,  
626 Messina JA, Maskarinec SA, Mueller-Premru M, Athan E, Tattevin P, Pericas JM, Woods  
627 CW, Otto M, Fowler VG. 2015. Clinical MRSA isolates from skin and soft tissue infections  
628 show increased in vitro production of phenol soluble modulins. *J Infect* 71:447–457.
- 629 20. Laabei M, Uhlemann A-C, Lowy FD, Austin ED, Yokoyama M, Ouadi K, Feil E,  
630 Thorpe HA, Williams B, Perkins M, Peacock SJ, Clarke SR, Dordel J, Holden M, Votintseva  
631 AA, Bowden R, Crook DW, Young BC, Wilson DJ, Recker M, Massey RC. 2015.  
632 Evolutionary Trade-Offs Underlie the Multi-faceted Virulence of *Staphylococcus aureus*.  
633 *PLOS Biol* 13:e1002229.
- 634 21. INFECT Study Group, Siemens N, Kittang BR, Chakrakodi B, Oppegaard O,  
635 Johansson L, Bruun T, Mylvaganam H, Arnell P, Hyldegaard O, Nekludov M, Karlsson Y,  
636 Svensson M, Skrede S, Norrby-Teglund A. 2015. Increased cytotoxicity and streptolysin O  
637 activity in group G streptococcal strains causing invasive tissue infections. *Sci Rep* 5.
- 638 22. Rosén A, Arnell P, Madsen MB, Nedrebø BG, Norrby-Teglund A, Hyldegaard O, dos  
639 Santos VM, Bergey F, Saccenti E, INFECT Study Group, Skrede S. 2018. Diabetes and  
640 necrotizing soft tissue infections-A prospective observational cohort study: Statistical analysis  
641 plan. *Acta Anaesthesiol Scand* 62:1171–1177.
- 642 23. Bouchiat C, Moreau K, Devillard S, Rasigade J-P, Mosnier A, Geissmann T, Bes M,  
643 Tristan A, Lina G, Laurent F, Piroth L, Aissa N, Duval X, Le Moing V, Vandenesch F,  
644 French VIRSTA Study Group. 2015. *Staphylococcus aureus* infective endocarditis versus  
645 bacteremia strains: Subtle genetic differences at stake. *Infect Genet Evol J Mol Epidemiol*  
646 *Evol Genet Infect Dis* 36:524–530.
- 647 24. Fey PD, Endres JL, Yajjala VK, Widhelm TJ, Boissy RJ, Bose JL, Bayles KW. 2013.  
648 A genetic resource for rapid and comprehensive phenotype screening of nonessential  
649 *Staphylococcus aureus* genes. *mBio* 4:e00537-00512.
- 650 25. Bae T, Schneewind O. 2006. Allelic replacement in *Staphylococcus aureus* with  
651 inducible counter-selection. *Plasmid* 55:58–63.
- 652 26. Diep BA, Chan L, Tattevin P, Kajikawa O, Martin TR, Basuino L, Mai TT, Marbach  
653 H, Braughton KR, Whitney AR, Gardner DJ, Fan X, Tseng CW, Liu GY, Badiou C, Etienne  
654 J, Lina G, Matthay MA, DeLeo FR, Chambers HF. 2010. Polymorphonuclear leukocytes  
655 mediate *Staphylococcus aureus* Panton-Valentine leukocidin-induced lung inflammation and  
656 injury. *Proc Natl Acad Sci U S A* 107:5587–5592.
- 657 27. Dickson MA, Hahn WC, Ino Y, Ronfard V, Wu JY, Weinberg RA, Louis DN, Li FP,  
658 Rheinwald JG. 2000. Human Keratinocytes That Express hTERT and Also Bypass a  
659 p16INK4a-Enforced Mechanism That Limits Life Span Become Immortal yet Retain Normal  
660 Growth and Differentiation Characteristics. *Mol Cell Biol* 20:1436–1447.
- 661 28. Yaffe D, Saxel O. 1977. Serial passaging and differentiation of myogenic cells  
662 isolated from dystrophic mouse muscle. *Nature* 270:725–727.
- 663 29. Bigot A, Duddy WJ, Ouandaogo ZG, Negroni E, Mariot V, Ghimbovski S, Harmon  
664 B, Wielgosik A, Loiseau C, Devaney J, Dumonceaux J, Butler-Browne G, Mouly V, Duguez  
665 S. 2015. Age-Associated Methylation Suppresses SPRY1, Leading to a Failure of Re-  
666 quiescence and Loss of the Reserve Stem Cell Pool in Elderly Muscle. *Cell Rep* 13:1172–  
667 1182.
- 668 30. Vilette D, Laulagnier K, Huor A, Alais S, Simoes S, Maryse R, Provansal M,  
669 Lehmann S, Andreoletti O, Schaeffer L, Raposo G, Leblanc P. 2015. Efficient inhibition of  
670 infectious prions multiplication and release by targeting the exosomal pathway. *Cell Mol Life*  
671 *Sci CMLS* 72:4409–4427.
- 672 31. Alais S, Soto-Rifo R, Balter V, Gruffat H, Manet E, Schaeffer L, Darlix JL, Cimarelli

673 A, Raposo G, Ohlmann T, Leblanc P. 2012. Functional mechanisms of the cellular prion  
674 protein (PrPC) associated anti-HIV-1 properties. *Cell Mol Life Sci* 69:1331–1352.  
675 32. Thorley M, Duguez S, Mazza EMC, Valsoni S, Bigot A, Mamchaoui K, Harmon B,  
676 Voit T, Mouly V, Duddy W. 2016. Skeletal muscle characteristics are preserved in  
677 hTERT/cdk4 human myogenic cell lines. *Skelet Muscle* 6.  
678 33. Trouillet S, Rasigade J-P, Lhoste Y, Ferry T, Vandenesch F, Etienne J, Laurent F.  
679 2011. A novel flow cytometry-based assay for the quantification of *Staphylococcus aureus*  
680 adhesion to and invasion of eukaryotic cells. *J Microbiol Methods* 86:145–149.  
681



TABLE 1 Quantification of intracellular bacteria assessed by transmission electron microscopy

<b>Cells</b>	<b>Strains</b>	<b>Number of analysed cells</b>	<b>Number of infected cells<sup>a</sup></b>	<b>Number of bacteria in infected cells<sup>a</sup></b>	<b>Mean number of bacteria per infected cells</b>	<b>Percentage of infected cells</b>
Myoblasts	INFECT2127	301	44	154	3,5	14.62
	SF8300	175	20	76	3.8	11.43
Keratinocytes	INFECT2127	455	13	45	3.46	2.86
	SF8300	491	7	26	3.7	1.43

<sup>a</sup>Assessed by visual counting of TEM sections

TABLE 2 Frequency of the genes detected by DNA microarray in *S. aureus* NSTI and BSI isolates<sup>a</sup>.

---

**Adhesins encoding genes**

Gene or allele	NSTI isolates (%) n = 9	RSI isolates (%) n = 21	P <sub>adjust</sub> <sup>(b)</sup>
<i>fnbA</i>	9 (100)	21 (100)	1.000
<i>fnbB</i>	6 (66.7)	19 (90.5)	1.000
<i>clfA</i>	9 (100)	21 (100)	1.000
<i>clfB</i>	9 (100)	21 (100)	1.000
<i>cna</i>	5 (55.6)	8 (38.1)	1.000
<i>spa</i>	9 (100)	21 (100)	1.000
<i>sdrC</i>	9 (100)	21 (100)	1.000
<i>sdrD</i>	7 (77.8)	20 (95.2)	1.000
<i>bbp</i>	5 (55.6)	21 (100)	0.156
<i>ebpS</i>	9 (100)	21 (100)	1.000
<i>map/eap</i>	7 (77.8)	20 (95.2)	1.000

**Toxins encoding genes**

<i>eta</i>	0 (0)	1 (4.8)	1.000
<i>etb</i>	0 (0)	0 (0)	1.000
<i>tst1</i>	2 (22.2)	3 (14.3)	1.000
<i>sea</i>	1 (11.1)	2 (9.5)	1.000
<i>seb</i>	2 (22.2)	0 (0)	1.000
<i>sec</i>	1 (11.1)	2 (9.5)	1.000
<i>sed</i>	0 (0)	5 (23.8)	1.000
<i>see</i>	0 (0)	0 (0)	1.000
<i>seg</i>	5 (55.6)	15 (71.4)	1.000
<i>seh</i>	1 (11.1)	0 (0)	1.000
<i>sei</i>	5 (55.6)	15 (71.4)	1.000
<i>sej</i>	0 (0)	5 (23.8)	1.000
<i>Superantigen</i> <sup>(c)</sup>	7 (77.8)	18 (85.7)	1.000
<i>lukS-PV</i>	1 (11.1)	0 (0)	1.000
<i>hla</i>	9 (100)	21 (100)	1.000
<i>hlb</i> <sup>123</sup> <sup>(d)</sup>	7 (77.8)	18 (85.7)	1.000
<i>func_hlb</i> <sup>(e)</sup>	0 (0)	0 (0)	1.000

**Other putative virulence factors encoding genes**

<i>icaA</i>	9 (100)	21 (100)	1.000
<i>chp</i>	8 (88.9)	15 (71.4)	1.000

**Regulation encoding genes**

<i>agrI</i>	6 (66.7)	7 (33.3)	1.000
<i>agrII</i>	1 (11.1)	10 (47.6)	1.000
<i>agrIII</i>	2 (22.2)	2 (9.5)	1.000
<i>agrIV</i>	0 (0)	2 (9.5)	1.000

---

<sup>a</sup>NSTI, Necrotizing Soft Tissue Infection; BSI, BloodStream Infection; <sup>b</sup>P-values are calculated for each gene or allele with a two-tailed Fisher's exact test. Bonferroni correction was applied; <sup>c</sup>At least one superantigen; <sup>d</sup>h1b123 represents *h1b* encoding gene alleles detected by one of the probes 1,2,3; <sup>e</sup>func\_h1b accounts for the *h1b* functional encoding gene.

TABLE 3 Description of clinical strains used in this study<sup>a</sup>

Species	Disease category	Clinical diagnosis	Site of isolation	Strain ID	CC or emm type	Source (ref)
<i>S. aureus</i>	Invasive	NSTI	Fascia	ST2014 <b>1878</b>	CC188	NRCS (this study)
	Invasive	NSTI	Fascia	ST2014 <b>0479</b>	CC8	NRCS (this study)
	Invasive	NSTI	Fascia	ST2014 <b>0899</b>	CC45	NRCS (this study)
	Invasive	NSTI	Fascia	ST2014 <b>1963</b>	CC30	NRCS (this study)
	Invasive	Extensive cellulitis	Blood	ST2015 <b>1186</b>	CC25	NRCS (this study)
	Invasive	NSTI	Subcutaneous tissue	INFECT <b>2023</b> /ST2017 <b>0477</b>	CC30	INFECT (this study)
	Invasive	NSTI	Subcutaneous tissue	INFECT <b>2127</b> /ST2017 <b>0479</b>	CC15	INFECT (this study)
	Invasive	NSTI	Subcutaneous tissue	INFECT <b>3045</b> /ST2017 <b>0482</b>	CC188	INFECT (this study)
	Invasive	NSTI	Blood	INFECT <b>6005</b> /ST2014 <b>0625</b>	CC45	INFECT (this study)
	Invasive	Endocarditis	Blood	ST2011 <b>1452</b>	CC5	(1)
	Invasive	Endocarditis	Blood	ST2010 <b>2292</b>	CC5	(1)
	Invasive	Endocarditis	Blood	ST2010 <b>1433</b>	CC97	(1)
	Invasive	Endocarditis	Blood	ST2009 <b>1672</b>	CC8	(1)
	Invasive	Endocarditis	Blood	ST2009 <b>1693</b>	CC45	(1)
	Invasive	Endocarditis	Blood	ST2009 <b>1729</b>	CC22	(1)
	Invasive	Endocarditis	Blood	ST2010 <b>0860</b>	CC30	(1)
	Invasive	Endocarditis	Blood	ST2010 <b>2139</b>	CC398	(1)
	Invasive	Endocarditis	Blood	ST2010 <b>2295</b>	CC5	(1)
	Invasive	Endocarditis	Blood	ST2011 <b>0560</b>	CC5	(1)
	Invasive	Endocarditis	Blood	ST2011 <b>1220</b>	CC121	(1)
	Invasive	Endocarditis	Blood	ST2011 <b>1368</b>	CC15	(1)
	Invasive	Bacteremia	Blood	ST2009 <b>1950</b>	CC8	(1)
	Invasive	Bacteremia	Blood	ST2009 <b>1954</b>	CC30	(1)
	Invasive	Bacteremia	Blood	ST2010 <b>1786</b>	CC45	(1)
	Invasive	Bacteremia	Blood	ST2010 <b>1791</b>	CC5	(1)
	Invasive	Bacteremia	Blood	ST2010 <b>2304</b>	CC121	(1)
	Invasive	Bacteremia	Blood	ST2011 <b>0552</b>	CC15	(1)
	Invasive	Bacteremia	Blood	ST2011 <b>1372</b>	CC5	(1)
	Invasive	Bacteremia	Blood	ST2012 <b>2026</b>	CC5	(1)
	Invasive	Bacteremia	Blood	ST2012 <b>2021</b>	CC5	(1)
<i>S. pyogenes</i>	Invasive	NSTI	Blood	INFECT <b>2006</b>	emm1	(2)
	Invasive	NSTI	Tissue	INFECT <b>2028</b>	emm3	(2)
	Invasive	NSTI	Wound	INFECT <b>5004</b>	emm28	(2)
	Invasive	NSTI	Wound Tissue	INFECT <b>5006</b>	emm1	(2)
<i>S. epidermidis</i>	Non invasive	Nose colonization	Nose	CCM2124		
<i>S. haemolyticus</i>	Non invasive	ND	Skin	CCM2737		
<i>S. hominis</i>	Non invasive	ND	Skin	DSM20328		
<i>S. lugdunensis</i>	Non invasive	Breast abscess	Axillary node	ATCC43809		
<i>S. saprophyticus</i>	Non invasive	UTI	Urine	CCM883		
<i>S. warneri</i>	Non invasive	ND	Skin	CCM2730		

<sup>a</sup>NSTI, Necrotizing Soft Tissue Infection; CC, Clonal Complex; emm, M protein gene; UTI, Urinary Tract Infection; ND, Not Determine

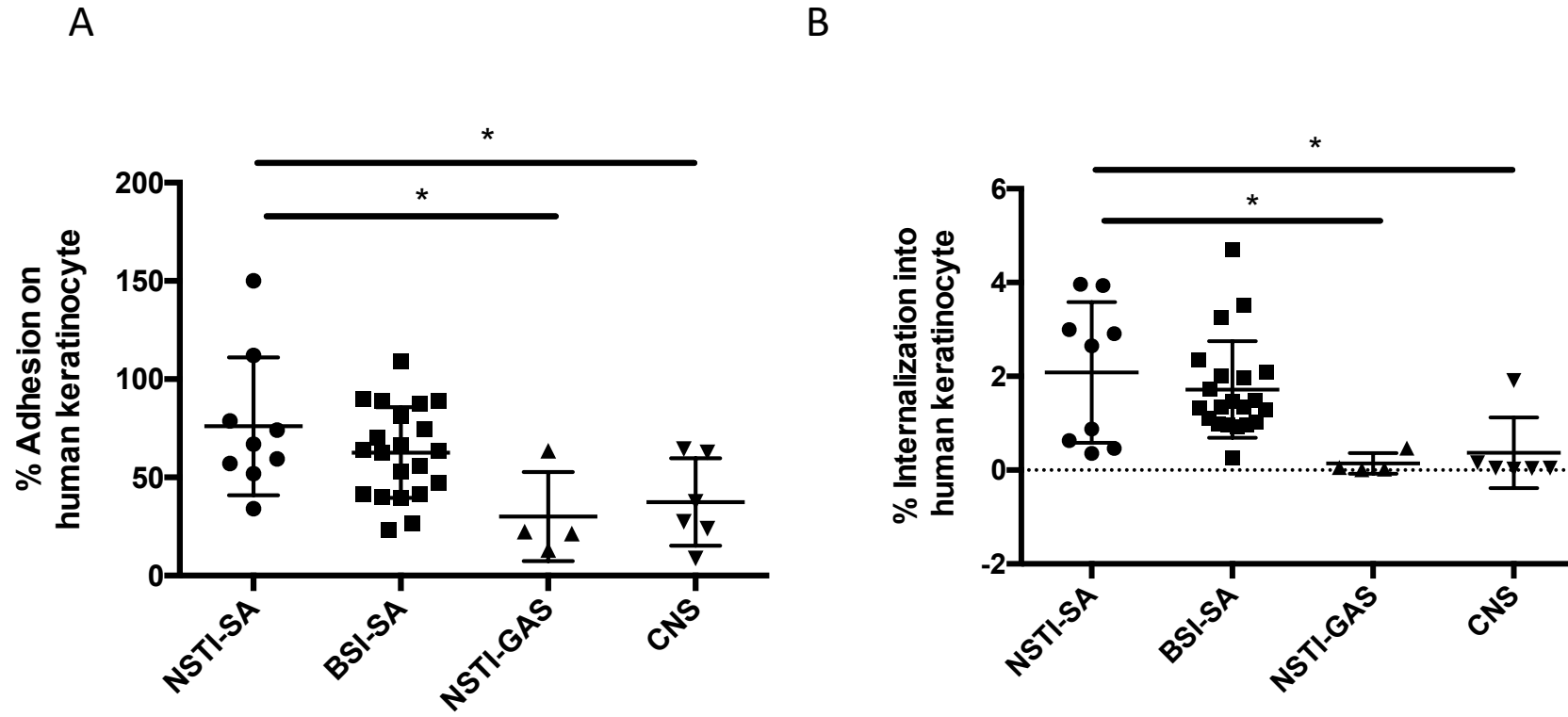


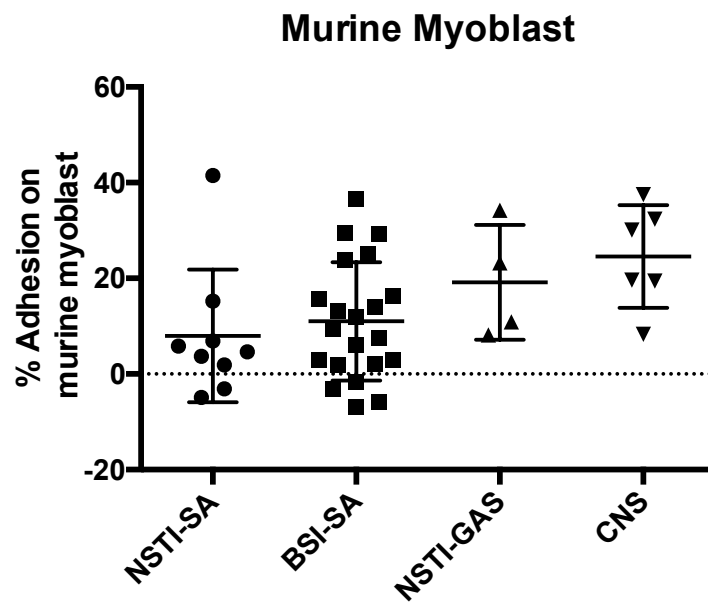
Fig.1

**Fig. 1. Adhesion and internalization of *Staphylococcus aureus* (SA), coagulase negative *Staphylococcus* (CNS) and group A *Streptococcus* (GAS) to human keratinocytes.** (A) Percentages of adhered bacteria were calculated after 2 hours of infection in relation to inoculum of infection. Intracellular bacteria assessed in B were subtracted; (B) Internalization was determined after 2 hours of infection followed by antibiotic treatment to exclude extracellular bacteria. Multiplicity of infection (MOI) = 10. The horizontal lines within each group represent the mean value  $\pm$  standard deviations of at least three independent experiments per strain. \* $p < 0.05$ , \*\* $p < 0.01$ , \*\*\*  $p < 0.001$ .

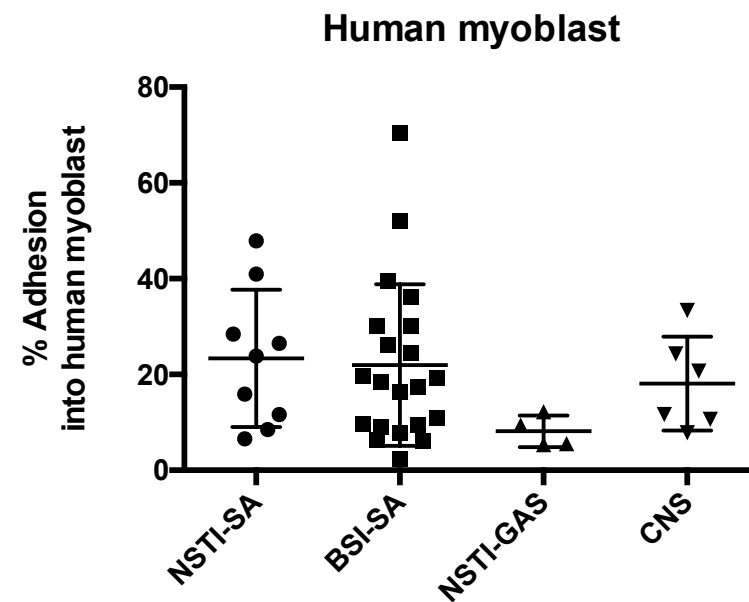
**Fig. 2. Adhesion and internalization of *Staphylococcus aureus* (SA), coagulase negative *Staphylococcus* (CNS) and group A *Streptococcus* (GAS) to murine and human myoblasts. (A and B)**

Percentages of adherent bacteria were calculated after 2 hours of infection in relation to inoculum of infection. Intracellular bacteria assessed in C and D were subtracted; (C and D) Internalization was determined after 2 hours of infection followed by antibiotic treatment to exclude extracellular bacteria. Multiplicity of infection (MOI) = 10. The horizontal lines within each group represent the mean value  $\pm$  standard deviations of at least three independent experiments per strain. \* $p < 0.05$ , \*\* $p < 0.01$ , \*\*\* $p < 0.001$ , \*\*\*\* $p < 0.0001$ .

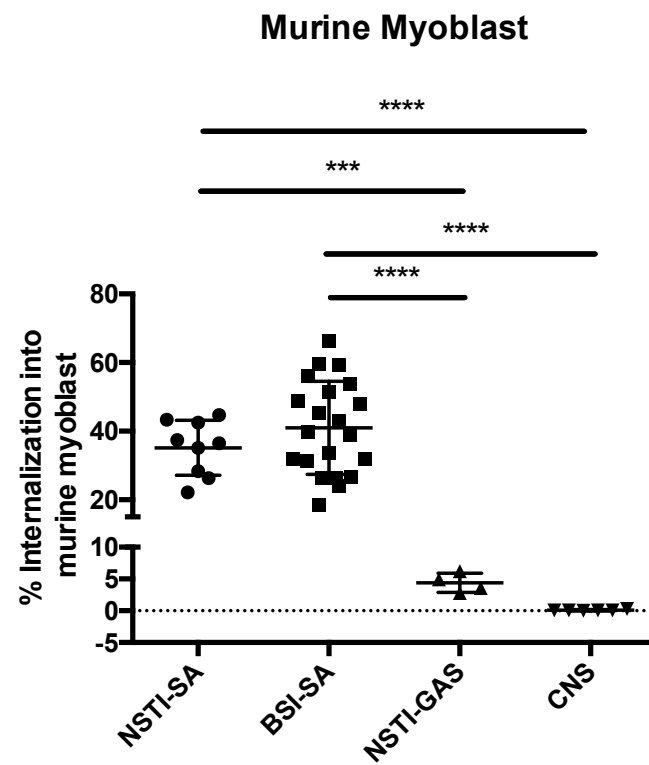
A



B



C



D

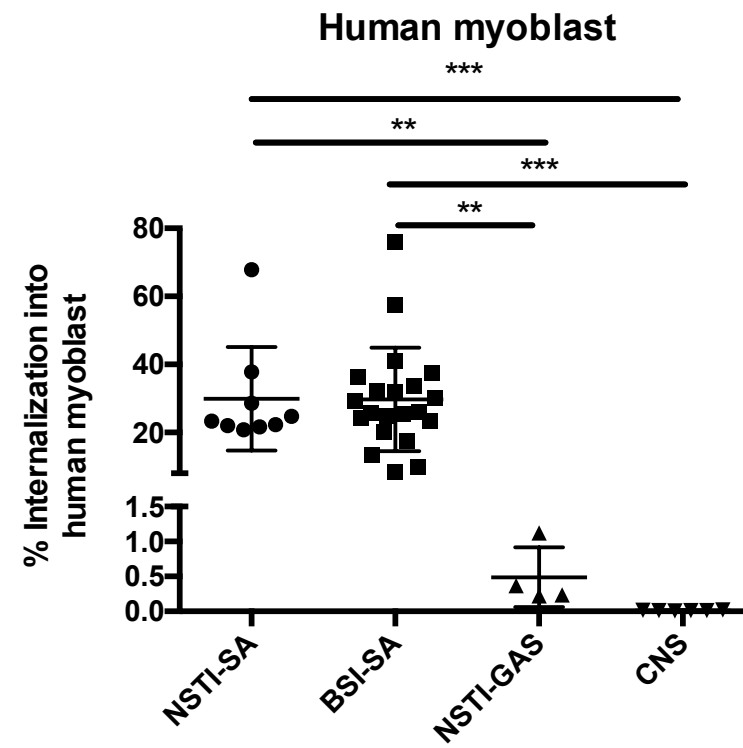
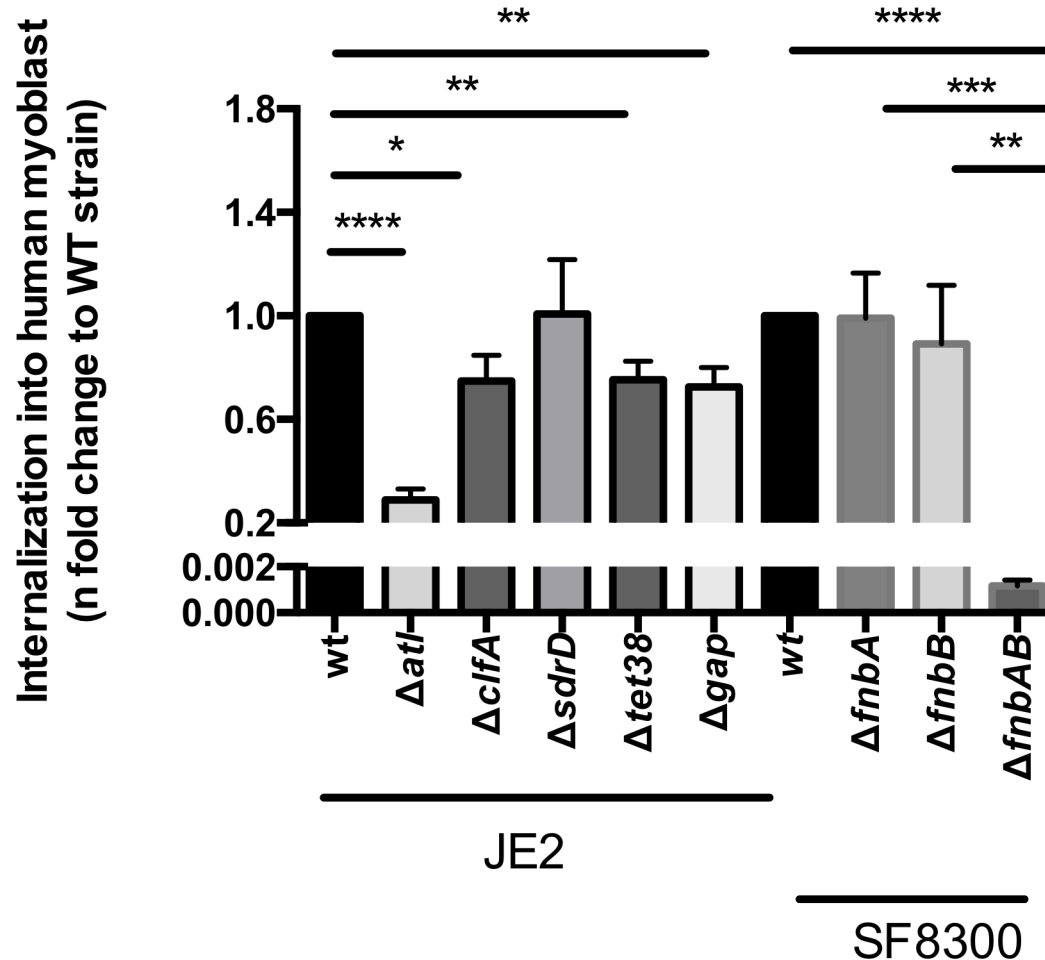


Fig.2

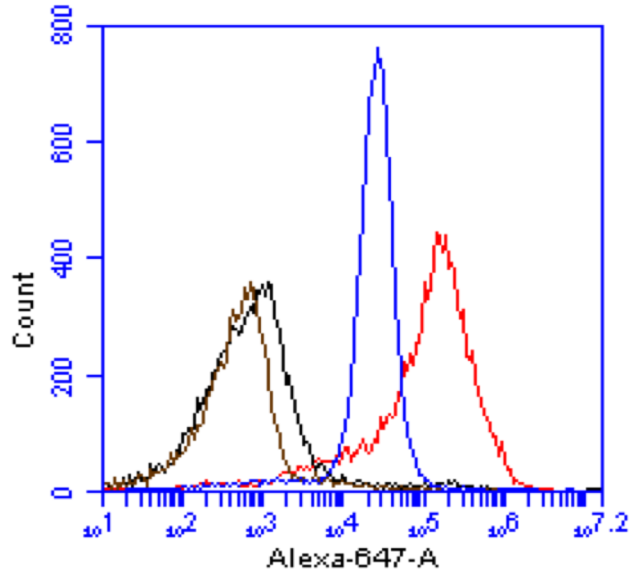




**Fig. 3. Internalization of *S. aureus* mutants into human myoblasts.** Internalization of the various mutants in genes encoding surface proteins was determined after 2 hours of infection followed by antibiotic treatment to exclude extracellular bacteria. The internalization was normalized to that of wild type strain. Multiplicity of infection (MOI) = 10. All values are means  $\pm$  standard error of mean of three independent experiments in duplicate for each strain. \*p<0.05, \*\*p<0.01, \*\*\* p<0.001, \*\*\*\*p<0.0001.

Fig.3

A



			MFI
Human myoblast	—	IgG control	7762
	—	Ac anti- $\alpha 5\beta 1$	244368

			MFI
Human keratinocyte	—	IgG control	983
	—	Ac anti- $\alpha 5\beta 1$	30011

B

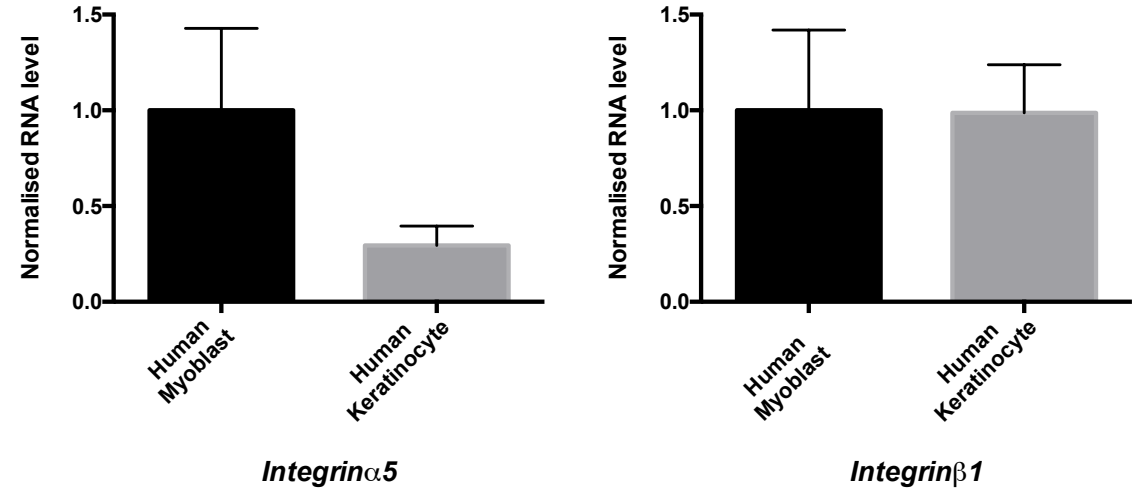


**Fig. 4. Expression of  $\alpha 5\beta 1$  integrin by human keratinocyte and myoblasts.** (A) Cell surface expression of  $\alpha 5\beta 1$  integrin assessed by flow cytometry and  $\alpha 5\beta 1$  antibody; (B) Relative transcript levels of  $\alpha 5$ ,  $\beta 1$  integrin sub-units were determined using quantitative reverse-transcriptase PCR, normalized to the internal  $\beta$ -actin standard. All values are means  $\pm$  standard error of mean of four independent experiments.

Fig.4

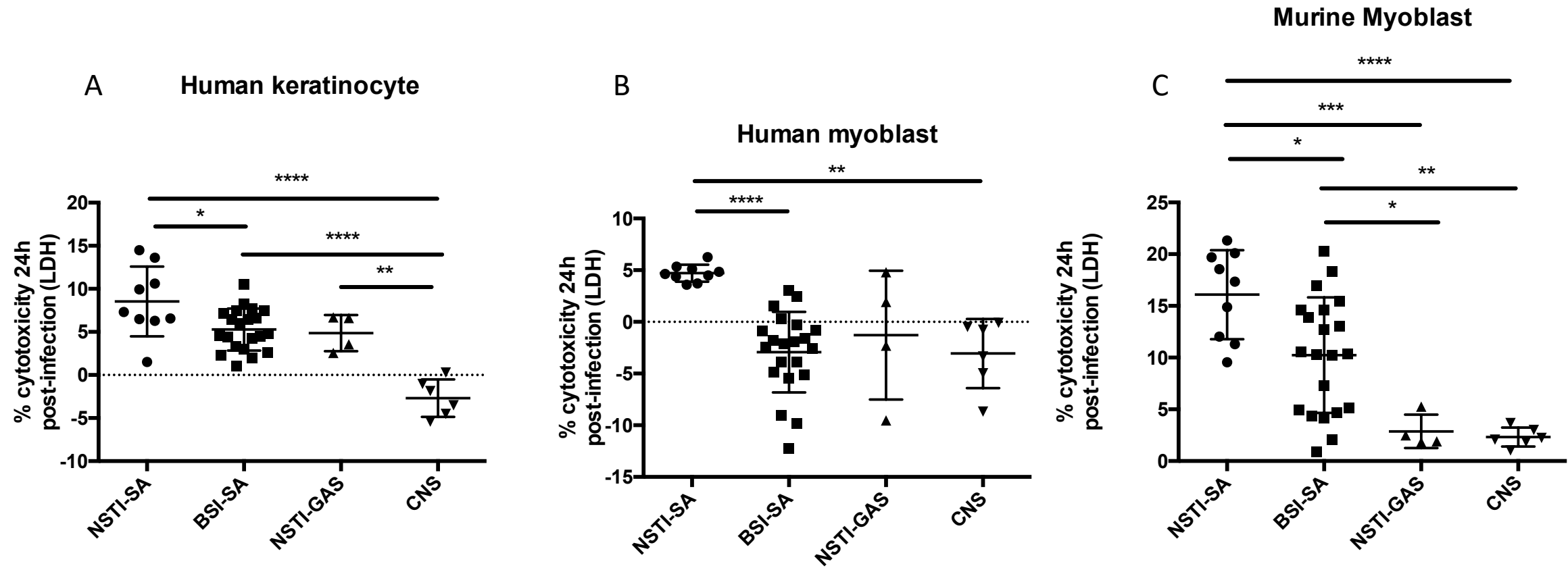


Fig.5

**Fig. 5. Cytotoxicity of intracellular bacteria at 24h post infection.** Cytotoxicity was estimated by quantifying LDH release by infected cells at 24 hours post infection. Multiplicity of infection (MOI) = 10. The percentage of cytotoxicity was calculated as follows:  $((\text{LDH infected cells} - \text{LDH lower control}) / (\text{LDH higher control} - \text{LDH lower control})) \times 100$ . The horizontal lines within each group represent the mean value  $\pm$  standard deviations of at least three independent experiments per strain. \* $p < 0.05$ , \*\* $p < 0.01$ , \*\*\*  $p < 0.001$ , \*\*\*\* $p < 0,0001$ .

**Fig. 6. Expression of intracellular bacterial mRNA into human myoblasts 3 hours post infection.** Relative transcript levels were determined using quantitative reverse-transcriptase PCR and expressed as n-fold change to the internal *hu* standard. The horizontal lines within each group represent the mean value  $\pm$  standard deviations. \* $p < 0.05$ , \*\* $p < 0.01$ .

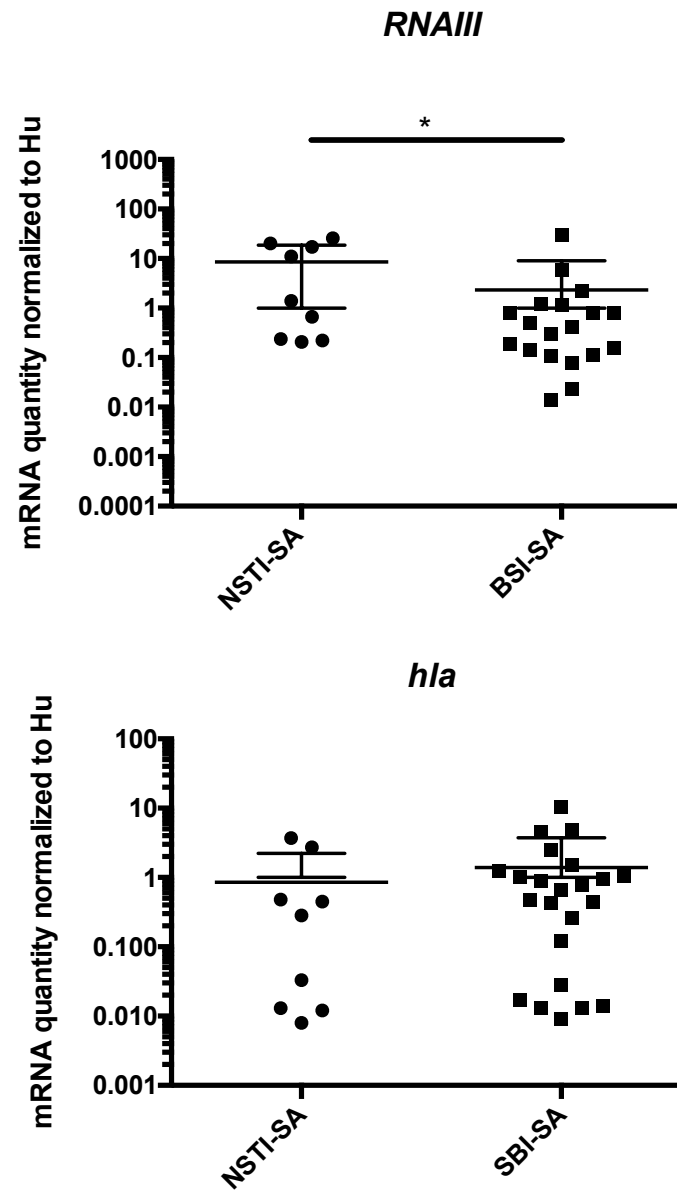
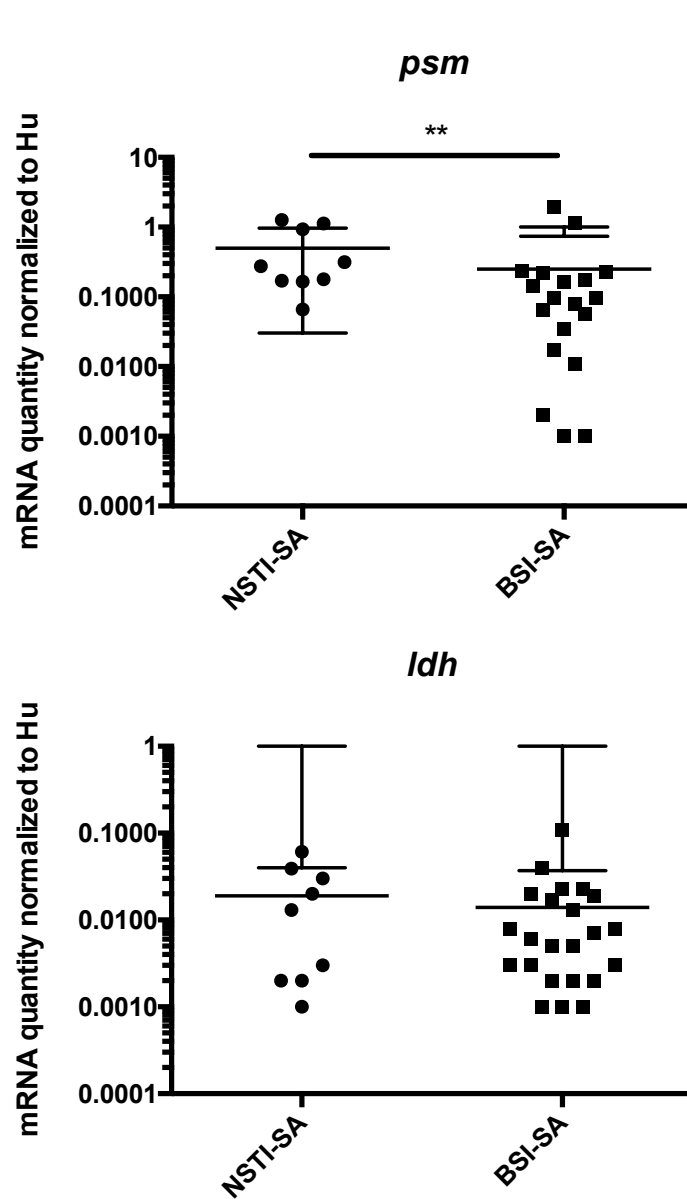


Fig.6